Supplement of Atmos. Chem. Phys., 15, 6205–6223, 2015
http://www.atmos-chem-phys.net/15/6205/2015/
doi:10.5194/acp-15-6205-2015-supplement

Atmospheric Chemistry and Physics Open Access

Supplement of

Quantifying sources, transport, deposition, and radiative forcing of black carbon over the Himalayas and Tibetan Plateau

R. Zhang et al.

Correspondence to: H. Wang (hailong.wang@pnnl.gov)

Table S1. The percentage contribution to global annual mean BC emissions from biomass-BB, biofuel-BB and FF sectors in each of the tagged source regions.

Source region	Biomass-BB (%)	Biofuel-BB (%)	FF (%)
ARC	0.07	0.00	0.04
NAM	0.72	1.04	4.36
CAM	1.37	0.55	1.25
SAM	4.82	0.90	2.88
EUR	0.19	1.11	6.35
NAF	0.01	0.32	1.14
SAF	15.75	4.47	0.89
MDE	0.00	0.03	1.18
CAS	0.22	0.02	0.43
SAS	0.65	5.56	2.58
EAS	0.64	5.70	15.30
SEA	5.22	2.49	2.40
PAN	1.81	0.06	0.47
RBU	2.11	0.23	2.66
HTP	0.00	0.08	0.09
ROW	0.03	0.00	1.78

Table S2. Global annual and seasonal mean lifetime (day) of BC emitted from the 32 tagged source regions/sectors, as well as from BB and FF sector over the whole globe (all source regions combined).

		DJF	MAM	JJA	SON	ANN
ARC	BB	2.2	3.0	4.7	3.9	4.5
	FF	2.1	1.9	1.6	1.4	1.7
NAM	BB	2.2	3.0	4.1	3.6	3.4
	FF	2.1	2.8	3.9	3.2	3.0
CAM	BB	2.6	4.9	2.8	1.7	3.9
	FF	3.5	5.0	2.4	2.3	3.3
SAM	BB	3.5	3.7	8.4	6.8	6.8
	FF	2.9	3.0	4.1	3.9	3.5
EUR	BB	2.0	2.7	6.4	4.0	4.0
	FF	1.9	2.5	4.9	2.9	3.1
NAF	BB	8.8	10.8	10.2	10.0	10.0
	FF	5.4	8.9	12.9	9.1	9.1
SAF	BB	9.3	6.1	5.1	7.1	7.2
	FF	4.4	4.1	4.3	3.9	4.2
MDE	BB	5.9	8.9	12.6	11.3	9.9
	FF	6.2	9.1	12.4	11.5	9.8
CAS	BB	2.8	4.7	7.5	4.7	5.9
	FF	2.7	5.4	9.7	5.8	5.9
SAS	BB	7.4	7.5	1.9	4.4	5.5
	FF	7.5	7.6	2.3	4.9	5.6
EAS	BB	3.2	3.6	2.5	3.1	3.1
	FF	3.1	3.3	2.4	3.0	2.9
SEA	BB	2.7	3.5	1.8	1.8	2.5
	FF	2.2	1.8	1.4	1.5	1.7
PAN	BB	5.7	4.5	5.6	6.8	6.1
	FF	4.2	3.3	2.5	2.9	3.2
RBU	BB	2.2	3.8	4.4	3.4	4.0
	FF	2.0	2.5	4.9	2.6	3.0
HTP	BB	6.6	6.0	4.0	6.5	5.8
	FF	6.1	6.2	4.9	6.4	5.9
ROW	BB	2.2	2.6	4.1	2.7	2.9
	FF	2.3	2.5	2.4	2.5	2.5
Globe	BB	6.9	5.0	4.6	5.2	5.4
	FF	3.1	3.6	3.8	3.5	3.5

Table S3. Concentration and deposition of BC and dust in snow/ice from an ice core drilled at Mt. Everest (27.7°N, 86.9°E) reported by Ginot et al. (2014) and evaluated by Ménégoz et al. (2014), where the monsoon season is defined as June-September and the inter-monsoon consists of the rest of eight months. The model grid cell is located northward (28.0°N, 86.9°E), where the altitude of the model surface is high enough to allow a continuous seasonal snow cover. Modeled concentrations represent the temporal average of the BC/dust concentrations in the top snow layer (i.e., a constant surface depth of 8 mm snow water in Ménégoz et al. (2014) and the top 2 cm of snowpack in this study). "N/A" means no snow in the model grid where the ice core located. All percentages are computed from the annual deposition values.

		Annual	Inter-monsoon	Monsoon	References
BC concentration ($ng\ g^{-1}$)	Observation	3.0	9.2	1.0	Ménégoz et al. (2014)
	Model	201	285	28	Ménégoz et al. (2014)
	Model	111.8	111.8	N/A	This study
BC deposition ($mg\ m^{-2}\ yr^{-1}$)	Observation	3.2	75%	25%	Ménégoz et al. (2014)
	Model	53	58%	42%	Ménégoz et al. (2014)
	Model	34.3	63%	37%	This study
Dust concentration ($mg\ kg^{-1}$)	Observation	10.1	11.1	10.1	Ménégoz et al. (2014)
	Model	10.4	13	5	Ménégoz et al. (2014)
	Model	4.4	4.4	N/A	This study
Dust deposition ($g\ m^{-2}\ yr^{-1}$)	Observation	10.1	28%	72%	Ménégoz et al. (2014)
	Model	6.4	60%	40%	Ménégoz et al. (2014)
	Model	3.8	59%	41%	This study

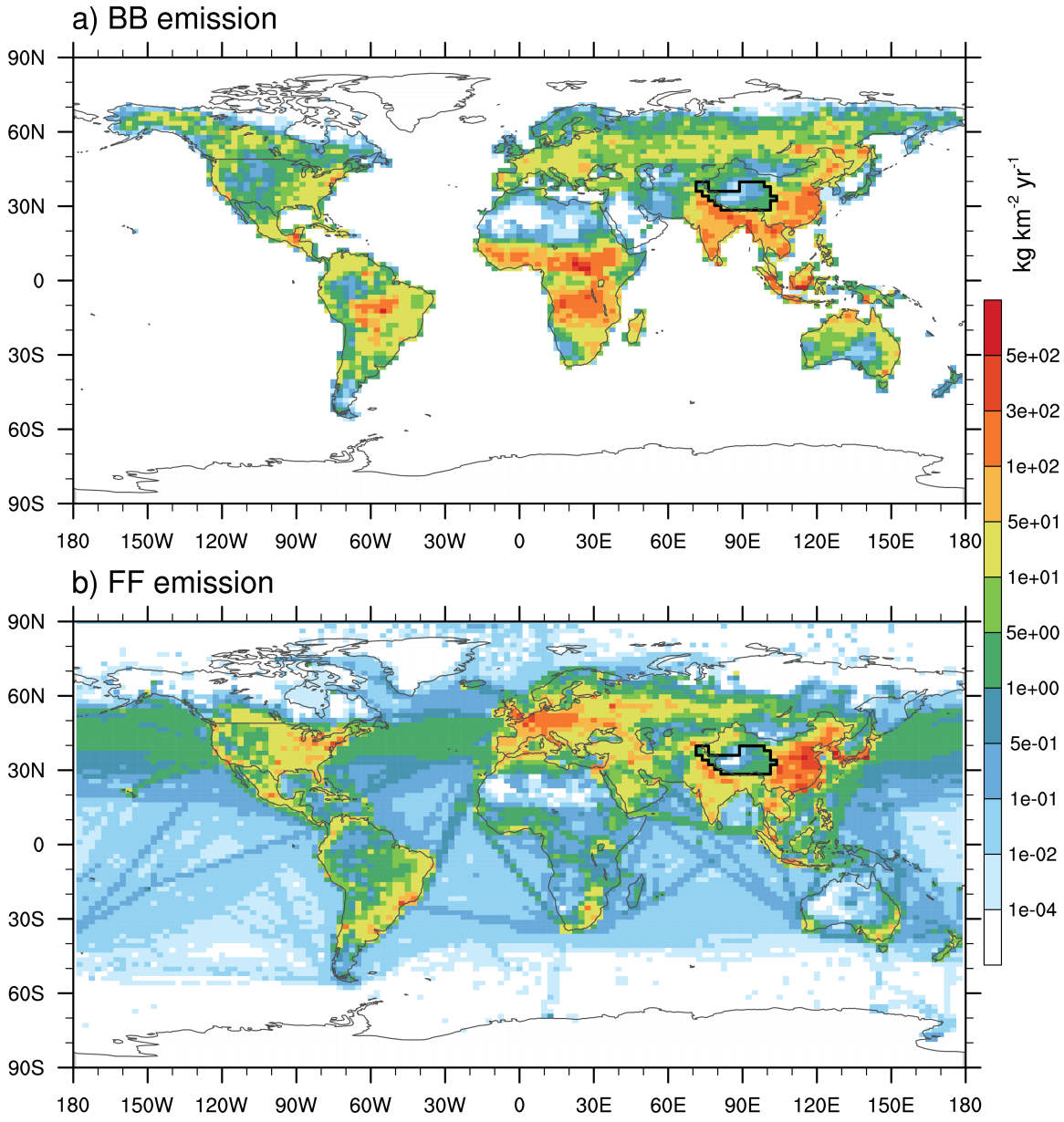

Fig. S1. Spatial distribution of BC annual mean emission rate from (a) BB and (b) FF sectors in the IPCC AR5 year-2000 emission inventory. HTP is marked with black outline.

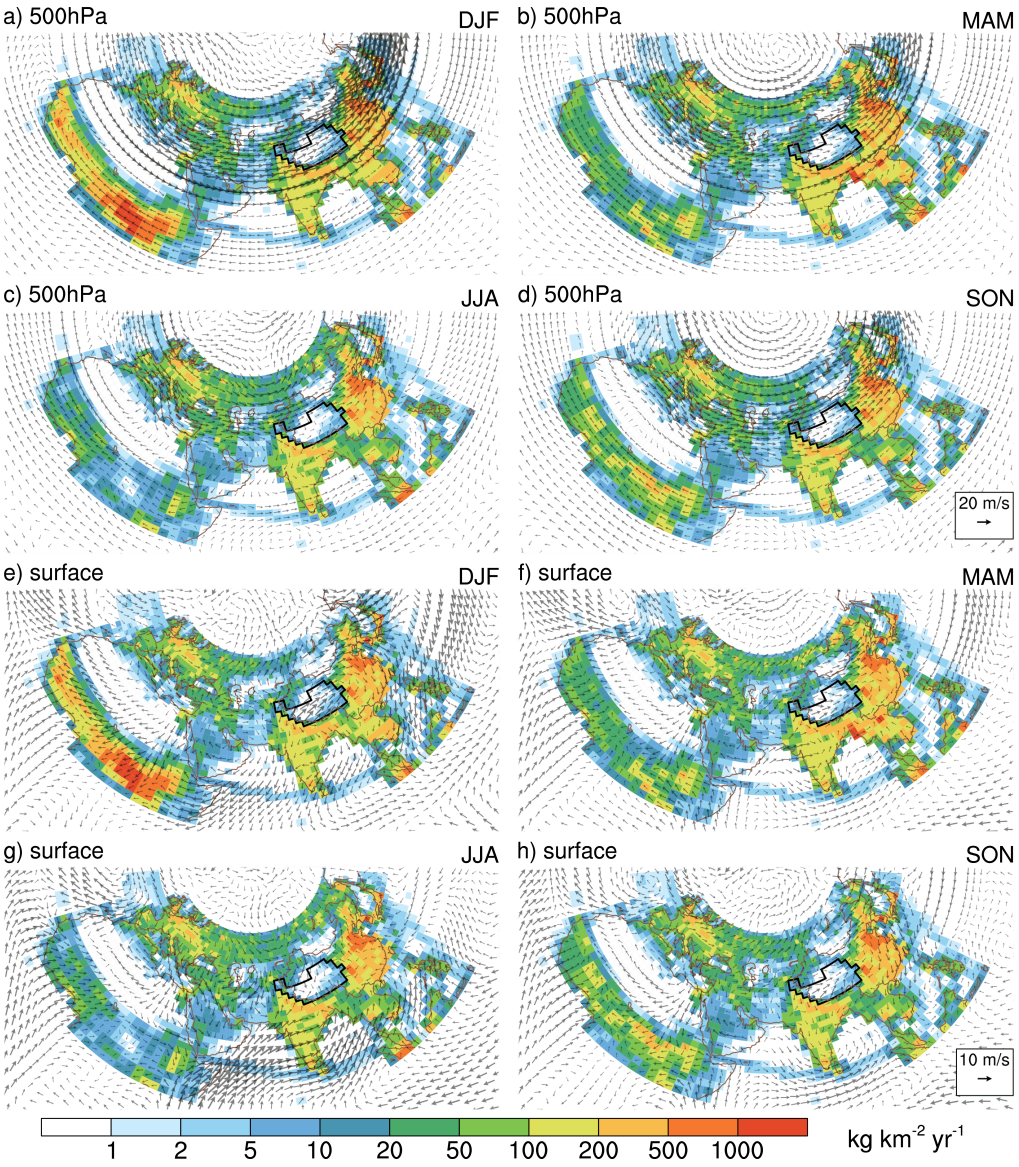

Fig. S2. Seasonal mean BC emission rates (in kg km^{-2} yr^{-1}, colors) in the AR5 year-2000 emission inventory, superimposed with horizontal wind vectors (denoted by arrows) at 500hPa (a−d) and at the surface (e−h, lowest layer of the model) from year-2001 MERRA reanalysis datasets used in the CAM5 simulation. The HTP is marked with black outline.

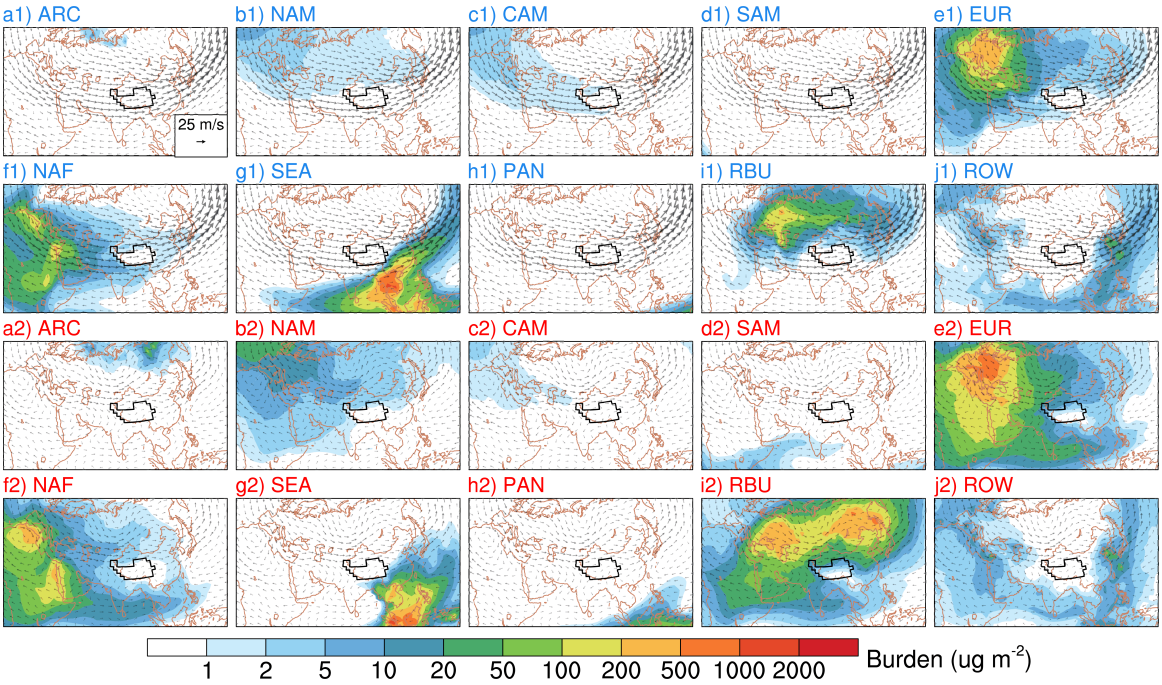

Fig. S3. Spatial distributions of seasonal mean BC (BB+FF) column burden (in μg m^{-2}, colors) for DJF (a1−j1) and JJA (a2−j2), respectively, originating from the ten tagged source regions (in addition to the six major ones shown in Fig. 4), superimposed with the corresponding seasonal mean horizontal wind vectors at 500hPa. The HTP is marked with black outline.

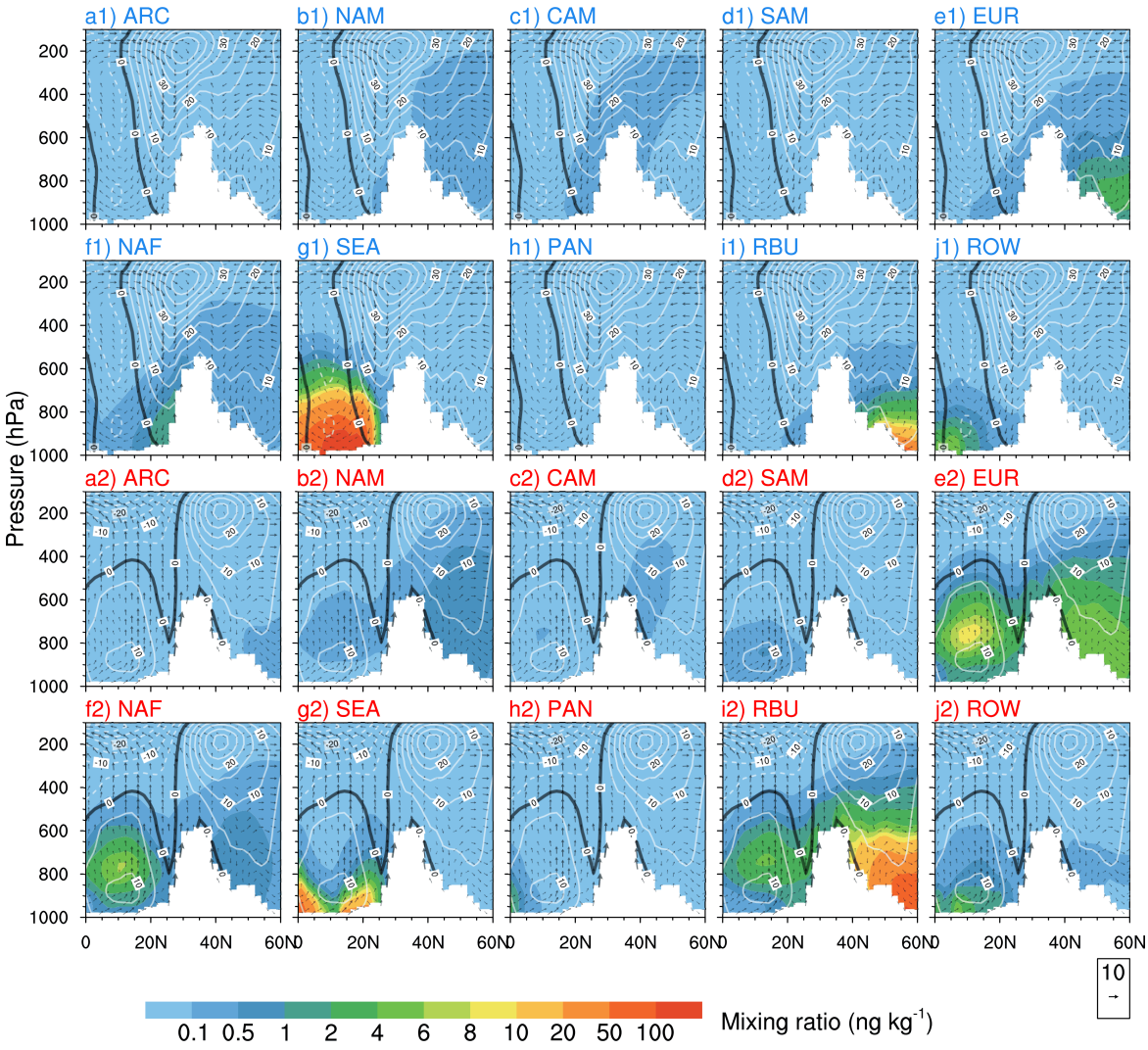

Fig. S4. Latitude-height distributions of seasonal mean BC (BB+FF) mass mixing ratios (in ng kg^{-1}, colors) averaged over the longitude band of 71.25−101.25° E for DJF (a1−j1) and JJA (a2−j2), respectively, originating from the ten tagged source regions (in addition to the six major ones shown in Fig. 4). The white shaded area denotes topography, and the superimposed white contours at intervals of 5 m s^{-1} represent the westerly (solid) and easterly (dashed) corresponding seasonal mean zonal winds over the same longitude band with the thick solid black contour at 0 m s^{-1}. The corresponding seasonal mean wind vectors (consisting of vertical velocity in units of -10^{-4} hPa s^{-1} and meridional wind in m s^{-1}) are represented by arrows.

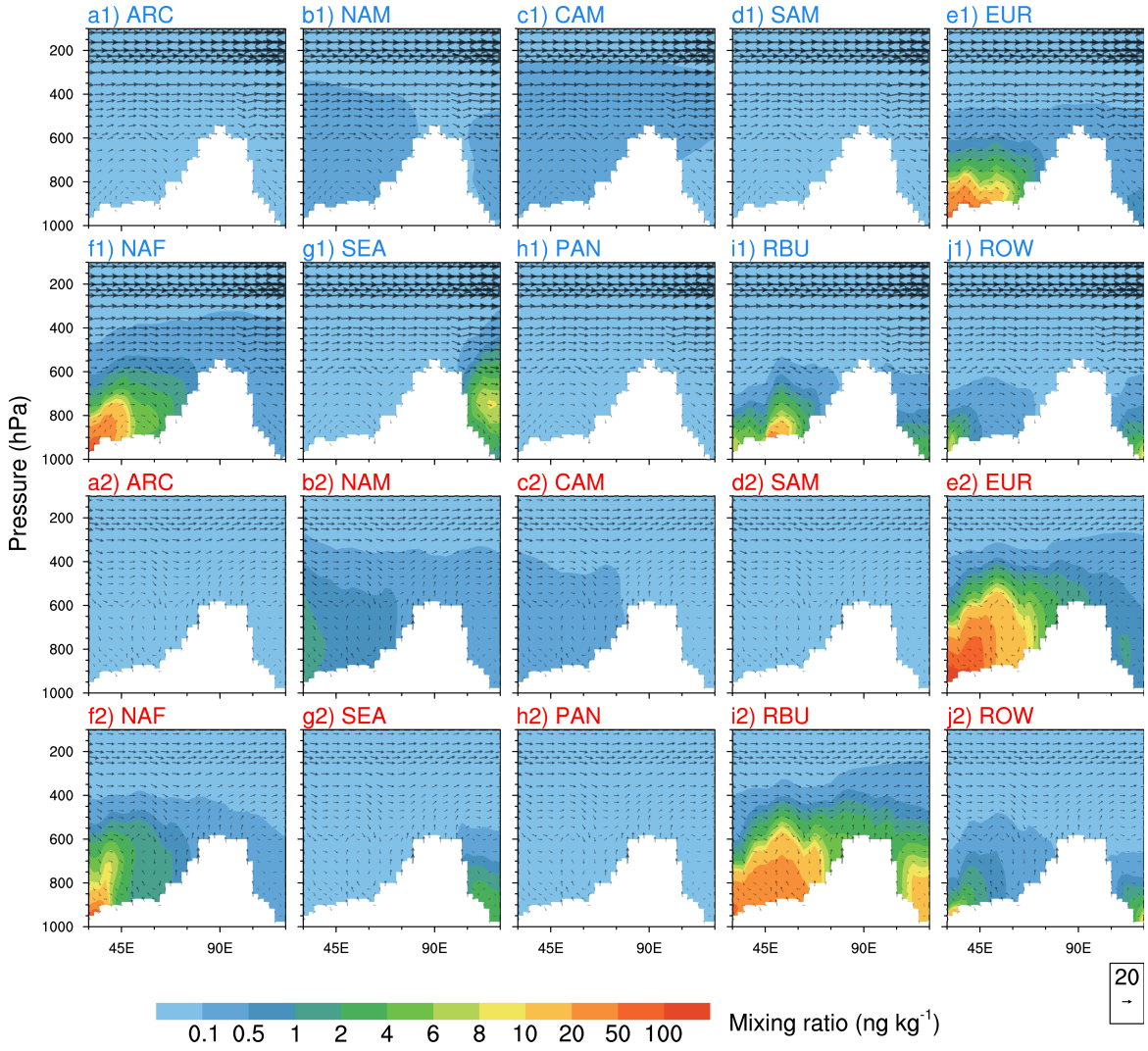

Fig. S5. Longitude-height distributions of seasonal mean BC (BB+FF) mass mixing ratios (in ng kg^{-1}, colors) averaged over the latitude band of 28−40° N for DJF (a1−j1) and JJA (a2−j2), respectively, originating from the ten tagged source regions (in addition to the six major ones shown in Fig. 4). The white shaded area denotes topography, and the superimposed arrows represent corresponding seasonal mean wind vectors (consisting of vertical velocity in units of -10^{-4} hPa s^{-1} and zonal wind in m s^{-1}).

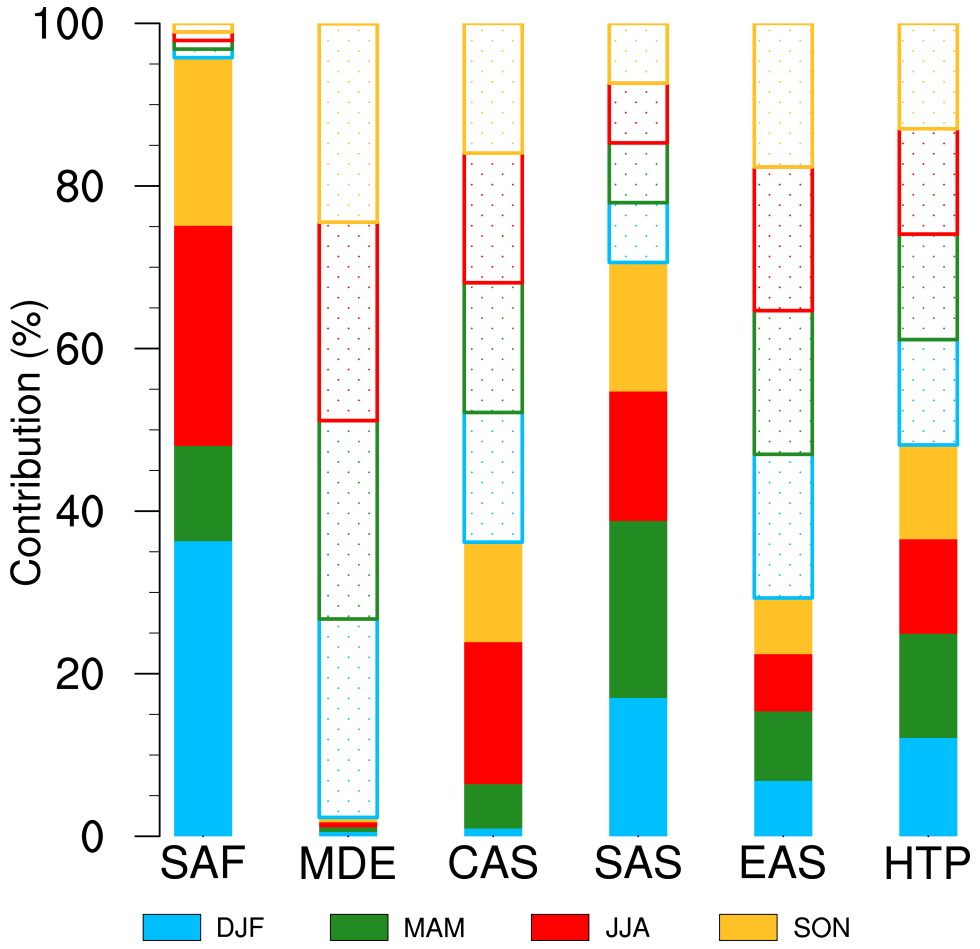

Fig. S6. Seasonal contribution to the annual total BC emissions from BB (solid pattern bar) and FF (dotted pattern bar) source sectors in each of the six source regions.